Quinacrine inhibits cMET-mediated metastasis and angiogenesis in breast cancer stem cells

Biswajit Das
Kalinga Institute of Industrial Technology (KIIT), Deemed to be University
Chinmayee Sethy
Kalinga Institute of Industrial Technology (KIIT), Deemed to be University
Subhajit Chatterjee
Kalinga Institute of Industrial Technology (KIIT), Deemed to be University
Somya Ranjan Dash
Kalinga Institute of Industrial Technology (KIIT), Deemed to be University
Saptarshi Sinha
Kalinga Institute of Industrial Technology (KIIT), Deemed to be University
Subarno Paul
Kalinga Institute of Industrial Technology (KIIT), Deemed to be University
Kunal Goutam
Acharya Harihar Regional Cancer Centre
Chanakya Nath Kundu (cnkundu@kiitbiotech.ac.in)
Kalinga Institute of Industrial Technology (KIIT), Deemed to be University

Research Article

Keywords: Breast cancer, Cancer stem cells, cMET, Quinacrine, Metastasis, Angiogenesis

Posted Date: April 25th, 2022

DOI: https://doi.org/10.21203/rs.3.rs-1576361/v1

Abstract

A trans-membrane receptor, mesenchymal-epithelial transition factor (cMET), is responsible for cancer metastasis and angiogenesis. A very little is known about the role of cMET in cancer stem cells (CSCs). Quinacrine (QC), a bioactive agent, has shown anti-CSCs activity. Here, the role of QC in deregulation of cMET-mediated metastasis and angiogenesis has been systematically evaluated *in vitro* in highly-metastatic-breast-CSCs (mBCSCs), *ex vivo* in patient-derived-breast-cancer-stem-cells (PDBCSCs) and *in vivo* in xenograft mice model systems. Cell proliferation, migration, invasion and representative metastasis markers were upregulated in cMET-overexpressed cells and QC exposure inhibited these processes in both mBCSCs and PDBCSCs. Interestingly, metastasis was inhibited after silencing of cMET and very less significant alteration of the process was noted in QC-treated cMET-silenced cells. Increased in vascularization, and cell-cell tube formation, and enhanced MMP2 and MMP9 enzymatic activities were noted after cMET-overexpression but these processes got reversed after cMET knockdown. In addition, QC inhibited angiogenesis after cMET-overexpression, but failed to change in cMET-silenced cells. Reduction of tumor volume and decreased expression of metastatic and angiogenic markers were also noted in xenograft mice after QC treatment. Furthermore, QC inhibited cMET activity by de-phosphorylation of its tyrosine residues (Y1234 and Y1356) and downregulation of its downstream cascade.

Introduction

Breast cancer is the second most common cancer worldwide and the leading cause of cancer related death in women [1] [2]. It has been commonly observed that even after successful therapeutic interventions, breast cancer often relapses [3]. This recurrence of cancer is due to the presence of cancer stem cells (CSCs), which comprise of a small subpopulation of cells within a tumor, and possess high self-renewal, drug efflux and DNA repair capabilities [4]. CSCs also promote tumor progression, highlighting their roles in different stages of cancer, which include metastasis [5], angiogenesis [6] and resistance to chemotherapy [7]. The conventional cancer treatments have failed to achieve success because they are unable to specifically target CSCs within the heterogeneous cancer cell population [7]. Hence, researchers are currently focussing on breast cancer stem cells (BCSCs) as a potential target for the development of novel breast cancer therapies [2] [4].

Mesenchymal-epithelial transition factor (cMET) is a cell-surface protein tyrosine-kinase, aberrantly expressed in various solid tumors, including breast cancer [8]. It comprises 50 kDa alpha-chain and 140 kDa beta-chain and is located on chromosome 7q21-31. It has a natural ligand, hepatocyte growth factor (HGF). Binding of HGF with cMET results in c-MET dimerization and trans-phosphorylation of the tyrosine residues in the intracellular domain [9]. Autophosphorylation of these domains leads to the activation of downstream signaling cascade [10]. Catalytic activation of downstream proteins regulates several cellular processes, including cancer cell survival, proliferation, motility, invasion, epithelial-to-mesenchymal transition (EMT), and angiogenesis [9] [10] [11]. A recent report had suggested that upregulation of cMET expression is significantly correlated with expression of the CSC markers like

CD133, CD44, and ALDH1 in BCSCs [12]. Although cMET is involved in tumor metastasis and angiogenesis in breast cancer [13], studies regarding the role of cMET in CSCs are limited. Among the different ways to inhibit c-MET, inhibition of autophosphorylation of c-MET has emerged as one of the major ways to develop an anti-cancer therapy [10].

Quinacrine (QC) is a plant-based, safe, bioactive compound, derived from quinine and has shown anti-cancer activity in different types of cancer, including breast cancer [14] [15] [16]. Previous studies suggest that QC inhibits cancer cell growth through various mechanisms such as arresting the cell cycle in the S-phase via inhibition of the topoisomerase activity, causing apoptosis, regulation of autophagy, inhibition of NF-kβ and Wnt-TCF signaling through adenomatous polyposis coli (APC) gene [14] [17] [18]. QC is a smart and highly efficient molecule and it specifically targets CSCs without harming normal cells [14] [19] [17] [20]. Early reports also suggested that QC has anti-metastatic and anti-angiogenic potentiality in cancer [14] but it needs further research to explore the detailed mechanism.

Earlier, conventional cMET-targeted chemotherapies exhibited a lot of side effects such as hypertension, loss of appetite, leukocytopenia, fatigue, and anorexia [21] [22]. Therefore, targeting cMET with a natural, bioactive and safe drug would be a plausible approach for an effective anti-CSCs therapy. Interestingly, a previous study indicated that QC is a tyrosine kinase inhibitor [23] and hence it is expected that there will be an effective inhibition of cMET in BCSCs upon treatment with QC. However, the role of QC in inhibition of cMET-mediated metastasis and angiogenesis in breast cancer has not been examined yet. Here, we have studied and analysed the underlying biochemical basis for the effect of QC on cMET-mediated metastasis and angiogenesis in breast cancer using *in vitro* (highly metastatic breast cancer stem cells; mBCSCs), *ex vivo* (patient derived breast cancer stem cells; PDBCSCs), and *in vivo* (xenograft mice), model systems.

Results

Cytotoxic potentiality of QC in highly metastatic breast cancer stem cells (mBCSCs)

To check the cytotoxic potentiality of QC in mBCSCs, the metastatic model from breast cancer cell lines, MCF-7 and MDA-MB-231, was developed. The formation of post-epithelial-to-mesenchymal-transition (PEMT) cells was pictorially represented for both the cell lines (**Fig. 1 Ai and Aii**). Next, to validate the metastatic model and CSCs properties of MCF-7-PEMT and MDA-MB-231-PEMT cells, the expression of the stemness markers was assessed by western blot analysis. There was a complete loss in the expression of E-cadherin (an epithelial marker) and increase in the expression of Vimentin (a mesenchymal marker) in mammosphere (MAMMO). Additionally, high E-cadherin and abolishment of Vimentin expressions in PEMT cells confirmed the development of a true metastatic model (**Fig. 1 Bi and Bii**). Moreover, a significant increase in the expression of stemness markers such as N-cadherin, CD-44 and CD-133 was observed in both MCF-7-PEMT and MDA-MB-231-PEMT cells compared to the parental cells (**Fig. 1 Bi and Bii**). The invasive potential of MCF-7-PEMT and MDA-MB-231-PEMT cells was found to be increased upto 60% and 75%, respectively ($P<0.0001$) compared to their parental cells (**Fig. 1 Ci**).

Next, the ELISA result showed a significant increase (4-fold, P<0.0001) in the expression of proliferation marker, Ki-67 in both PEMT cells compared to their parental cells (**Fig. 1 Cii**). Further, the expression of stemness markers (CD-44 and CXCR-4) in both PEMT cells was found to be higher (P<0.0001) compared to their respective parental cells (**Fig. 1 Ciii and Civ**). Next, MTT cell viability assay was performed and IC_{50} values of QC in MCF-7-PEMT and MDA-MB-231-PEMT cells were found to be 8μM and 9μM, respectively (**Fig. 1 Di and Dii**).

Anti-metastatic and anti-angiogenic potentialities of QC in mBCSCs cells

Next, the anti-metastatic and anti-angiogenic properties of QC were evaluated in MDA-MB-231-PEMT cells [24]. ELISA results showed a significant decrease (P<0.0001) in the representative metastasis markers such as CXCR-4, CD-44, ALDH-1 and Oct-4 after QC treatment (**Fig. 1 Ei-iv)**. Similarly, the levels of selective angiogenesis markers such as Ang1, Ang2, VEGF-A and HIF-1α were also significantly reduced (P<0.0001) upon the QC treatment (**Fig. 1 Ev-viii)**. Further, western blot analysis also revealed a significant decrease in the expression of metastatic markers, including CXCR-4 (5-fold), CD-44 (3.3-fold), ALDH-1 (1.6-fold) and Oct-4 (1.4-fold) as well as angiogenesis markers, including Ang1 (2-fold), Ang2 (3.3-fold), VEGF-A (3.3-fold) and HIF-1α (2.5-fold) after 9μM of QC treatment in comparison to control (**Fig. 1 F**).

cMET is associated with metastasis and angiogenesis in mBCSCs

Western blot analysis was performed to check the levels of cMET in MCF-7-PEMT and MDA-MB-231-PEMT cells. There was a 4.4-fold increase in cMET expression in MDA-MB-231-PEMT cells as compared to MCF-7-PEMT cells (**Fig. 2A**). Next, to decipher the role of cMET in metastasis and angiogenesis, cMET was overexpressed in MCF-7-PEMT (relatively lower expression of cMET in comparison to MDA-MB-231-PEMT cells) and silenced in MDA-MB-231-PEMT (relatively higher expression of cMET in comparison to MCF-7-PEMT) cells. In western blot analysis, cMET overexpressed (cMET-OE) MCF-7-PEMT cells showed a 5.2-fold increase in the expression of cMET compared to control, whereas cMET expression was diminished in cMET knocked-down (cMET-KD) MDA-MB-231-PEMT cells compared to control (**Fig. 2B**). Then to measure the proliferation rate of these cells, the MTT assay was performed. A significant increase (2-fold, P<0.0001) in proliferation rate was noticed in cMET-OE-MCF-7-PEMT cells compared to control (MCF-7-PEMT cells). On the other hand, a 2.4-fold decrease (P<0.0001) in proliferation rate was observed in cMET-KD-MDA-MB-231-PEMT cells compared to its parental counterpart (**Fig. 2C**).

Further, to understand the role of cMET in metastasis and angiogenesis, the expression of representative metastatic and angiogenic markers was evaluated in both cMET-OE and cMET-KD cells in comparison to parental cells. Interestingly, increased expression of metastatic markers, such as CXCR-4 (1.9-fold), CD-44 (1.5-fold), ALDH-1 (1.9-fold), and Oct-4 (2.5-fold) was observed in cMET-OE-MCF-7-PEMT cells, whereas a noticeable reduction of 1.25-, 1.4-, 1.6- and 1.4-fold was observed in cMET-KD-MDA-MB-231-PEMT cells compared to their respective control (**Fig. 2D**). Similarly, an increase in the expression of angiogenic markers, such as Ang1 (2.5-fold), Ang2 (2.1-fold), VEGF-A (2.1-fold) and HIF-1α (1.8-fold), in cMET-OE-

MCF-7-PEMT cells and reduction of 2.5-, 1.6-, 2-, and 2.5-fold, respectively in cMET-KD-MDA-MB-231-PEMT cells were observed with respect to their parental control (**Fig. 2D**).

Next, to know the effect of QC on the metastatic and angiogenic markers, the cells were treated with respective IC_{50} concentrations of QC. When cMET-OE-MCF-7-PEMT cells were treated with QC (8μM), the expression of representative metastatic markers (CXCR-4 and CD-44) and angiogenic markers (Ang1 and VEGF-A) were decreased approximately to 1.6-fold compared to untreated control **(Fig. 2E)**. On the other hand, when cMET-KD-MDA-MB-231-PEMT cells were exposed to QC (9μM), the expression of the metastatic markers was found to be decreased upto 1.4-fold compared to untreated control (**Fig. 2E**).

In addition, the proliferation rate was found to be significantly reduced (2-fold, $P<0.0001$) in cMET-OE-MCF-7-PEMT cells after QC (8μM) treatment. But a relatively low amount of reduction (1.6-fold, $P<0.05$) in proliferation rate was found in cMET-KD-MDA-MB-231-PEMT cells upon treatment with QC (9μM) **(Fig. 2F).**

QC deregulated cMET-mediated metastasis and angiogenesis

A systematic study was carried out to determine the role of QC on cMET-mediated metastasis and angiogenesis. Since, migration and invasion are the major hallmarks of cancer [25], cell migration assay and matrigel invasion assay were performed to investigate the metastatic potentiality of cMET-OE-MCF-7-PEMT cells and cMET-KD-MDA-MB-231-PEMT cells after QC treatment. It was observed that increasing concentration of QC reduced the migration rate of these cells. The cMET-OE-MCF-7-PEMT cells exhibited better migration ability than MCF-7-PEMT cells **(Fig. 2 Gi).** On the other hand, cMET-KD-MDA-MB-231-PEMT cells showed comparatively less migration ability than MDA-MB-231-PEMT cells **(Fig. 2 Gii)**. But cell migration ability was reduced with the increasing concentration of QC in all conditions **(Fig. 2 G).**

Next, the invasive potentiality of cMET-OE-MCF-7-PEMT and cMET-KD-MDA-MB-231-PEMT cells and their fate after QC (with respective IC_{50}) treatment were examined. The invasive potentiality was found to be significantly increased (1.3-fold, $P<0.0001$) in cMET-OE-MCF-7-PEMT cells and reduced (1.8-fold, $P<0.0001$) in cMET-KD-MDA-MB-231-PEMT compared to control (**Fig. 2H**). But, after treatment with QC (8μM), a 2-fold reduction ($P<0.0001$) in cell invasion was noted in cMET-OE-MCF-7-PEMT cells, while only a 1.2-fold reduction ($P<0.05$) was found when cMET-KD-MDA-MB-231-PEMT cells were treated with QC (9μM) (**Fig. 2 H**).

Then, *in ovo* CAM assay was performed to check the blood vessel formation following the addition of different CM (100μg/5 ml egg fluid) to the CAM (**Fig. 2 I**). A significantly higher amount of vascularization was observed when eggs were incubated with the CM of cMET enriched cells (cMET-OE-MCF-7-PEMT and MDA-MB-231-PEMT) compared to CM of cMET-KD-MDA-MB-231-PEMT and MCF-7-PEMT cells. But when eggs were incubated with CM of QC treated cells, the average vascularization was not significantly induced **(Fig. 2 Ii-Iix)**. The bar graph represents the average vascularization in different conditions (**Fig. 2 Ix**).

It is well known fact that endothelial cell proliferation increases in response to angiogenic stimuli. Therefore, to check the role of QC in cMET-induced tube-formation, HUVECs were incubated with different types of CM (100 µg/3ml) as mentioned in figure 2J. A characteristic growth pattern of HUVECs was found after 72 h of CM addition. It was noticed that the average tube length was significantly increased (approximately 6-fold, P<0.0001) when HUVECs were incubated with CM of cMET enriched cells (cMET-OE-MCF-7-PEMT and MDA-MB-231-PEMT), compared to untreated control. Additionally, CM from MCF-7-PEMT cells and cMET-KD-MDA-MB-231-PEMT cells showed a 3.8 fold and 2-fold increase in average tube length of HUVECs, respectively compared to untreated control (**Fig. 2J**). Then, to check the effect of QC in tube formation of HUVECs, CM of QC treated cells was added. It was noted that tube formation was not significant when HUVECs were incubated with QC treated CM in comparison to untreated control **(Fig. 2 J)**. The bar graph represents the average tube-length in different types of CM treated conditions (**Fig. 2 Ji**).

Next, the representative angiogenic markers, MMP-9 and MMP-2, were monitored by performing gelatin zymography. The CMs were collected from different types of CM-induced HUVECs culture and subjected to gelatin zymography as mentioned in **figure 2K**. Higher expression of MMP-9 and MMP-2 was noticed when HUVECs were incubated with CM of cMET-OE-MCF-7-PEMT and MDA-MB-231-PEMT cells in comparison to that observed when incubated with the CM of cMET-KD-MDA-MB-231 and MCF-7-PEMT cells **(Fig. 2 Ki).** The expression of MMP-9 and MMP-2 was not significantly changed when HUVECs were incubated with the CM of QC treated cells **(Fig. 2 Kii).**

Molecular mechanism of cMET inhibition by QC

Till now, the effect of QC in cMET-mediated metastasis and angiogenesis was studied. Next, to study the underlying mechanism of QC-mediated cMET inhibition in BCSCs, specific experiments were carried out. Phosphorylation of cMET is the key step for activating the downstream proteins in this signaling cascade [26]. Therefore, the expression of cMET, its intracellular domain phospho-cMET (p-cMET-Y1234 and p-cMET-Y1356) and the downstream signaling proteins were assessed by western blotting after treating the MDA-MB-231-PEMT cells with increasing concentrations of QC (**Fig. 3A**). Interestingly, unaltered expression of cMET at the basal level was observed after treatment with QC (**Fig. 3A**). However, a 3.5- and 5-fold decrease in the levels of p-cMET-Y1234 and p-cMET-Y1356, respectively, were observed after exposure with 9 µM QC. Additionally, other downstream proteins of cMET signaling cascade also got downregulated after QC exposure.

Immunofluorescence assay of p-cMET after QC treatment was also performed to confirm the above findings. Upon QC treatment, a dose-dependent reduction (P<0.0001) in the expressions of p-cMET-Y1234 and p-cMET-Y1356 was noted (**Fig. 3B**). The bar graph represents the reduction (P<0.0001) in the relative mean intensity of p-cMET expression with increasing concentrations of QC, in comparison to control (**Fig. 3 Bi and Bii**).

In addition, similar type of p-cMET immunofluorescence assay was carried out using cMET-KD-MDA-MB-231-PEMT cells as well. Here, a significantly lower expression of p-cMET (Y1234 and Y1356) in control

was observed, but upon QC treatment, the expression of cMET was abolished. **(Fig. 3C)**. The bar graph represents the reduction ($P<0.0001$) in the relative mean intensity of p-cMET expression with increasing concentrations of QC with respect to control (**Fig. 3 Ci and Cii**).

Clinical significance of cMET and QC-mediated reduction of metastasis and angiogenesis in PDCSCs cells

To delineate the clinical significance of cMET in breast cancer, malignant human breast cancer tissues of different grades (Grade I, II and III) along with their adjacent normal tissues were collected and processed for experimentation. The hematoxylin and eosin (H&E) stained slides suggested the cancerous nature or invasive histology with increasing grades of cancer tissue compared to uniform well differentiated histology of normal tissue (**Fig. 4 Ai**). The immunohistochemistry (IHC) result showed a significant increase in cMET expression with the increasing cancer grades (**Fig. 4 Aii**). An increased expression of cMET with increasing grades of cancer was also observed in western blot analysis. Notably, a 2.2-fold increase in cMET expression was observed in Grade-III tissue lysate compared to Grade-I tissue lysate (**Fig. 4B**).

Next, the isolated cells from Grade III tumor tissues were cultured and grown as adherent monolayer following the development of the metastatic model to generate PDBCSCs (**Fig. 4C**). To characterize the metastatic model, expressions of E-cadherin and Vimentin as well as other stem cell markers were checked at different stages of the model in patient derived breast cancer primary cells. Notably, very low expression of E-cadherin and a higher expression of Vimentin were observed in MAMMO (**Fig. 4D**). Additionally, the expression of other representative stemness markers (N-cadherin, CD-44 and CD-133) were significantly increased (>2-fold) in breast cancer primary PEMT cells (**Fig. 4 D**). Moreover, the rate of invasion (4-fold) and proliferation (2-fold) as well as the expressions of CXCR4 (2-fold) and CD-44 (2-fold) were also found to be elevated in breast cancer primary PEMT cells compared to control (primary breast cancer cells) (**Fig. 4 Ei–iv**). These breast cancer primary PEMT cells were referred to as PDBCSCs. Next, these cells were exposed to increasing concentrations of QC and IC_{50} concentration was found to be 5μM (**Fig. 4F**).

Finally, to examine the expression of several metastatic and angiogenic markers as well as cMET, p-cMET and the downstream proteins in PDBCSCs, the cells were treated with increasing concentrations of QC (0, 1, 3, 5, 7 and 9 μM) and processed for western blot analysis. Inspite of treatment with increasing concentrations of QC, the basal cMET expression remained unchanged in PDBCSCs. Interestingly, a 10-fold decrease in the expression of p-cMET (Y1234 and Y1356) was observed after 5μM of QC exposure with respect to untreated control (**Fig. 4G**). Similarly, the expression of other representative metastatic markers (CXCR-4, ALDH-1), angiogenic markers (Ang1, VEGF-A) and downstream signaling proteins (STAT3, FAK, PI3K, AKT, mTOR) of cMET got downregulated in PDBCSCs after treatment with QC in a dose-dependent manner as compared to untreated control (**Fig. 4 G).**

QC reduces metastasis and angiogenesis in mice xenograft model

To check the anti-metastatic and anti-angiogenic potentiality of QC *in vivo*, the mice xenograft model was developed using female BALB/c mice. Tumor formation was noticed after 10 days of breast cancer primary PEMT cells implantation. Day by day, the body weight of the mice significantly decreased and tumor volume was increased (P<0.0001) (**Fig. 5 A & B**). Notably, after QC treatment, a recovery in lost body weight and reduction of tumor volume was found (P<0.0001) (**Fig. 5 A & B**). Then, after sacrificing the mice, the tumor tissues were collected for further experiments. H&E staining revealed normal and cancerous histology of mice tissue (**Fig. 5 C**). Next, in IHC, overexpression of cMET, p-cMET (Y1234 & Y1356), metastatic markers (CD-44 and CXCR-4) and angiogenic markers (Ang1 and VEGF-A) in tumor tissues was observed. However, upon QC treatment, the expression of above mentioned metastatic and angiogenic markers got reduced compared to untreated tumor tissue but the expression of cMET was unchanged (**Fig. 5 D**).

Further, the mice tumor tissues were lysed and processed for western blotting. In western blot analysis, a similar result was observed, i.e., upon QC treatment, there was no change in the basal cMET level but there was a significant reduction in the expression of p-cMET (p-cMET-Y1234 & p-cMET-Y1356), metastatic markers (CXCR-4, CD-44), angiogenic markers (Ang1, VEGF-A) and downstream signaling proteins (STAT-3, FAK, PI3K, AKT, mTOR) of cMET compared to untreated control (**Fig. 6 E**).

Discussion

Although cMET has been used as a potential target for cancer therapy, numerous side effects and lack of specificity of the drugs limited the effectiveness of cMET-targeted anti-cancer therapy. A plant-based, bioactive agent, QC has anti-CSCs potentiality and found to exhibit anti-tyrosine kinase activity [14] [23]. In the present study, it was found that QC inhibited the cMET-induced metastasis and angiogenesis by de-phosphorylating autoregulatory domain of cMET and downregulating the downstream signaling cascade. For concluding this observation, we have systematically performed several biochemical assays using *in vitro*, *in ovo*, *ex vivo*, and *in vivo* model systems as follows;

1. First, the highly-metastatic-BCSCs (mBCSCs) model of MCF-7 and MDA-MB-231 cells was developed and characterized by several biochemical assays. Similar to the earlier reports [20], our data also suggest that the PEMT cells exhibit CSCs properties and can be referred to as CSCs **(**Fig. 1A, B, and **C)**.
2. The expression of representative metastatic markers (CXCR-4, CD-44, ALDH-1, and Oct-4) and angiogenic markers (Ang1, Ang2, VEGF-A and HIF-1α) was decreased after QC treatment in MDA-MB-231-PEMT cells in a dose-dependent manner (Fig. 1D, E, and **F**). Data appeared that QC might have anti-metastatic and anti-angiogenic potentialities in mBCSCs.
3. Overexpression of cMET is significantly associated with poor survival of breast cancer patients, especially in the triple-negative breast cancer (TNBC) subgroup [27]. Due to the increased expression of cMET in MDA-MB-231 cells, these cells are highly invasive, compared to MCF-7 cells [24] [28]. In our findings, the relatively lower expression of cMET in MCF-7-PEMT and higher expression in MDA-MB-231-PEMT cells support the above agreement. Additionally, the proliferation rates, and the

expression of representative metastatic and angiogenic markers were higher in cMET-OE cells than in its parental cells, whereas the opposite results were found in cMET-KD cells (Fig. 2A-D). In cMET-KD cells, the decrease in the rate of proliferation and the levels of representative metastatic and angiogenic markers after QC treatment (with respective IC_{50} concentrations) was much less significant in comparison to that observed in cMET-OE cells (Fig. 2E **and F).** This suggests that QC is plausibly acting through the inhibition of cMET.

4. Next, the crucial role of QC in the inhibition of cMET-mediated migration and invasion was examined. The cMET-OE cells showed higher migration ability than cMET-KD cells. But QC inhibits the cell migration of cMET-OE cells more significantly than that observed in cMET-KD cells in a dose-dependent manner (Fig. 2G**).** Next, the matrigel invasion assay also supported the above observation (Fig. 2H). Thus, it appeared that cMET might be played a pivotal role in cell migration and invasion of mBCSCs, which can be inhibited by QC.
5. It is a well-known fact that cMET promotes the secretion of important angiogenic factors and inhibition of cMET is believed to exert an anti-angiogenic effect on tumor cells [29]. To further investigate the role of QC on cMET-mediated angiogenesis, a series of experiments have been conducted. In *in ovo* CAM assay, CM from cMET enriched cells (cMET-OE-MCF-7-PEMT and MDA-MB-231 PMET) significantly induced the vascularization in CAM, whereas comparatively less vascularization was found when CM from cMET-KD-MDA-MB-231-PEMT and MCF-7 PMET cells were added. On the other hand, when the CM from the QC treated cancer cells were added to the CAM there was no significant vascularization observed (Fig. 2I; **Ii to Iix)**. Thus, cMET is responsible for inducing vascularization, which can be inhibited by QC in *in ovo* CAM assay. Similarly, tube-formation assay (Fig. 2J **& Ji)** and gelatin zymography (Fig. 2 **Ki and Kii**) also support the above findings. Thus, QC has a crucial role in the deregulation of cMET-mediated angiogenesis.
6. Next, the question arises that how QC is inhibiting cMET. For this, some specific experiments were carried out. The obtained results revealed that the cMET level was unchanged and the expression of p-cMET (Y1234 & Y1356) and downstream signaling proteins was decreased with the increasing concentrations of QC (Fig. 3A). The immunofluorescence data also supports the above observation (Fig. 3B **and C)**. Thus, data suggested that QC is acting through inhibition of the phosphorylation of cMET without altering its basal level. Taken together data suggested that QC inhibited the metastasis and angiogenesis process in *in vitro* BCSCs cells.
7. Now the question arises that whether QC also affects these processes in the tumor microenvironment (TME, where many types of cell population are present) similar to BCSCs? To address the question, we have carried out the experiments using the ex vivo model of patient derived breast cancer cells. The clinical significance of cMET was also analyzed and it was observed that the expression of cMET was enhanced with increasing grades (Grade-III > Grade-II > Grade-I) of breast cancer patient samples (Fig. 4A **and B).** Next, a patient-derived breast cancer stem cells (PDBCSCs) model was developed and validated, where PEMT cells were shown to be exhibiting CSCs properties (Fig. 4C **D E).** A significant reduction was observed in the expression of metastatic and angiogenic markers, p-cMET (Y1234 and Y1356), and downstream signaling proteins of cMET after treating the PEMT cells with increasing concentrations of QC while the basal cMET level was unaltered (Fig. 4F

and G). Thus, QC can effectively not only inhibit cMET-mediated metastasis and angiogenesis in BCSCs but also affects PDBCSCs.

8. Next, to further investigate these phenomena in the animal model, an *in vivo* xenograft mice model was developed. *In vivo* data also showed reduction of tumor volume along with other metastatic and angiogenic markers, p-cMET (Y1234 and Y1356) and unaltered expression of cMET after QC treatment (Fig. 5). Thus, QC exhibits anti-metastatic and anti-angiogenic effect in *in vitro*, *ex vivo* as well as *in vivo* model systems through inhibition of cMET.
9. Based on the above observations, we have schematically depicted the role of QC in inhibiting cMET and cMET-mediated metastasis and angiogenesis (Fig. 6**)**. Briefly, ligand binding leads to receptor dimerization and activation of cMET. After that, the representative downstream metastasis and angiogenesis-related proteins get upregulated, and ultimately, the metastasis and angiogenesis processes are induced. But after the administration of QC, it dephosphorylates and inactivates cMET. As a result, the downstream signaling proteins of cMET along with the metastatic and angiogenic factors get downregulated, and the de-phosphorylated cMET inhibits the metastasis and angiogenesis processes.

Conclusively, in this study, the role of QC in cMET-mediated metastasis and angiogenesis in breast cancer was investigated in pre-clinical model systems and it was found that QC has excellent anti-metastatic and anti-angiogenic activities through inhibition of cMET. But further research is required in clinical settings to ensure the application of this agent in human body to stop cancer progression.

Materials And Methods

Cell culture and reagents

The human breast cancer cell lines, MCF-7 (ATCC cat # HTB-22), MDA-MB-231 (ATCC cat # HTB-26), the human umbilical vein endothelial cells (HUVECs) and patient-derived breast cancer cells were cultured and grown for different experimentation, according to the previously described method [30] [31] . Cell culture reagents were purchased from HIMEDIA, India. QC (Cat #Q3251) and 3-(4, 5-dimethylthiazol-2yl)-2, 5-diphenyl tetrazolium bromide (MTT) were purchased from Sigma Chemical Co. (St Louis, MO). Human-specific cMET-siRNA (cat #sc-29397) and non-targeting (scrambled) siRNA (cat #sc-37007) were purchased from Santa Cruz Biotechnology® (Santa Cruz, CA, USA). The cMET plasmid pMD-Met (RefSec: NM_000245.2, Vector: pMD18-T Simple) (cat# HG10692-M) was purchased from Sino Biological, China. Antibodies were purchased from Elabscience®, USA and used for experimentation.

Development of metastatic model in breast cancer cell lines

The highly metastasis breast cancer model was developed according to the protocol mentioned earlier [30]. In brief, MCF-7 and MDA-MB-231 cells were trypsinized and resuspended in serum-free media supplemented with 10 ng/ml basic fibroblast growth factor (bFGF), 20 ng/ml epidermal growth factor (EGF), 5 µg/ml insulin, 0.4% bovine serum albumin (BSA) and 200 µM $CoCl_2$. The cells were stable till 7-8

passages and grew as an adherent monolayer. This phase of the cells was reported as Quiescent (Q) [30]. Prolonged culture of Q cells under a similar type of condition leads to the formation of mammospheres (MAMMO), which in turn formed a stable monolayer of the adherent immortal stem-like cells when put into serum-containing media. These cells were termed as 'post epithelial to mesenchymal transition' (PEMT) cells. Next, characterization and validation of the developed model system were carried out and the developed metastatic models were used for further experimental purposes.

Development of CSCs enriched metastatic model from breast cancer primary tumor cells

Breast primary tumor tissues were collected and processed for the formation of the metastatic model following the protocol mentioned earlier [30]. Briefly, breast tumor samples (invasive duct carcinoma) were collected from Acharya Harihar Regional Cancer Centre, Cuttack, Odisha, as per the Hospital Review Board, under ethical guidelines of the hospital. Tumor tissues were processed for the formation of the metastasis model. Briefly, the tumor tissues were washed in 1XPBS and chopped into tiny pieces in a media which contained a mixture of antibiotics (0.14mM ampicillin, 0.26μM Amphotericin B and 7.54 μM ciprofloxacin). After this it was treated with 0.1% collagenase along with 50U/mL dispase. Next, the sample was incubated in 37°C water bath for at least 2 h with continuous rotating motion. Then the cells were sieved through 40μm cell strainer to remove the fat cells, centrifuged at 1000 rpm for 10mins, seeded onto 60mm dishes in DMEM-F12 containing 20% FBS, 1.5mM L-glutamine and 2% antibiotic (100U/mL penicillin and 10mg/mL streptomycin) and allowed to grow for 5 to 8 days under regular observation. Then the metastatic model from patient-derived breast cancer cells was developed using the procedure described above and after characterization of these cells used for experimentation.

Preparation of Conditioned Media (CM)

According to the protocol discussed earlier, conditioned media were collected from the cultured MCF-7-PEMT, MDA-MB-231-PEMT, HUVECs etc. [32]. Briefly, 1 $\times 10^6$ cells were seeded in 60 mm sterile cell culture dishes and incubated for 48 h. On the other hand, different types of breast cancer cells were seeded followed by QC treatment after 24 h. These QC treated cells were incubated for another 48 h from the starting point of the drug administration. Then the media was collected from different conditions of cells and centrifuged at 1800 rpm at 4°C for 3-5 min. Then the supernatant was kept in a fresh tube and concentrated by using Eppendorf Concentrator plus (Eppendorf, Hamburg, Germany). The final concentrated liquid product was used as conditioned media (CM) in different biochemical assays and preserved at -20°C.

Measurement of cell proliferation and viability by MTT assay

The cell viability of QC-treated cells was measured by performing an MTT assay as described earlier [33]. Briefly, exponentially growing MCF-7-PEMT, MDA-MB-231-PEMT, CM induced HUVECs and primary PEMT cells (8000-10,000 cells/well) were seeded in 96 well culture plates and allowed to grow for 70-80% confluency. After the treatment with increasing concentrations of QC (0-10μM) for 48 h, 0.05% MTT was added to each well and incubated at 37°C for 5-7 h to form formazan crystals. Next, the formazan

crystals were dissolved with 0.2% NP-40 detergent. Then the color intensity was measured by a microplate spectrophotometer (Berthhold, Germany) at 570 nm wavelength. Similarly, the proliferation rate of cMET overexpressed (OE) MCF7-PEMT and cMET knockdown (cMET-KD) MDA-MB-231-PEMT cells was evaluated and compared them to their respective control.

ELISA to measure the proliferation, metastatic and angiogenic markers

According to our previously described protocol [33], an indirect enzyme-linked immunosorbent assay (ELISA) was performed to determine the expression of the cell proliferation marker Ki-67, the metastatic and stem cell markers (ALDH-1, CXCR-4, CD-44 and Oct-4) and angiogenesis markers (Ang1, Ang2, VEGF-A and HIF-1α) in respective cell lines after treating with increasing concentration QC (0, 5, 7, 9, 11, 13 μM) for 48 h. Briefly, 30 μg of protein antigen (CM) are well mixed with coupling buffer coated onto a 96 well microplate (#3679, Corning, NY, USA). Excess antigen-binding sites are blocked by using a blocking solution. Specific primary antibodies were added to detect the desired antigens followed by HRP conjugated secondary antibodies. The color was developed by adding ABTS substrate solution and the color intensity was measured at 405nm using a microplate reader (Berthold, Germany).

Western blot analysis

Western blot experiment was performed according to the protocol described earlier [34]. The tissue or cell lysate was prepared by using RIPA lysis buffer then SDS-PAGE was used to separate 80μg of protein samples which were then transferred to PVDF membrane for detection. Specific antibodies were applied to detect the protein of interest. Relative fold change in protein expression levels was measured by densitometry analysis by using a UVP GelDoc-IT® 310 system and represented as numerical values above each protein band panel. In all experiment of western blotting GAPDH served as loading control. The numbers above each blot represent fold changes in protein expression.

Knockdown of cMET in MDA-MB-231-PEMT cells

Endogenous cMET expression was silenced in MDA-MB-231 PEMT cells (high cMET expressing cell) using a siRNA tranfection protocol described earlier [34]. Briefly, we have transfected 0.25 μg cMET siRNA and an equal amount of scrambled siRNA (control) using a Lipofectamine-2000® transfection reagent (Thermo-Fischer Scientific, MA, USA). cMET knockdown (cMET-KD) was validated by Western blotting.

Overexpression of cMET in MCF-7-PEMT cells

cMET was transiently overexpressed in MCF-7-PEMT (low cMET expressing cell) cells as per the protocol described earlier [34]. cMET was transiently overexpressed in MCF-7-PEMT (low cMET expressing cell) cells via transfection of 4μg cMET pMD-Met plasmid by using a Lipofectamine-2000® transfection reagent. cMET overexpression (cMET-OE)was validated by Western blotting.

Matrigel invasion assay to check the invasion potentiality of cells

Matrigelinvasion assaywas performed according to the protocol described previously [33]. In short, $3x10^5$ cells were suspended in 100µL of serum-free media and seeded in a 24 well transwell plate (#3422, Corning, NY, USA), coated with 20 µL of matrigel (#356,234, BD Biosciences, CA, USA). Next, serum-containing media was added to the lower chamber and incubated for 24h. Accordingly, cells were treated with respective IC_{50} value of QC for 48 h prior to experiment. The non-invaded cells were removed with cotton swabs and the invaded cells were fixed with 4% paraformaldehyde followed by DAPI. Stained cells were counted at 20X magnification in 5 different fields under the inverted fluorescence microscope (Nikon, Tokyo, Japan). The percentage of the invaded cells was calculated and plotted in the graph.

Wound healing assay to check the cell migration

Cell migration potentiality in cMET-OE-MCF-7-PEMT and cMET-KD-MDA-MB-231-PEMT cells with or without the exposure of QC was examined by using a wound healing assay as described earlier [17]. Briefly, cells were cultured in 35 mm tissue culture dishes until 90% confluent. A sterile 20µL micro tip was used to make a straight-line scratch in the cell monolayer across the centre of the plate. The cells were treated in fresh media with respective concentration of QC and then the cells were left to migrate in the medium for another 30 h. Photos were captured by an inverted bright field microscope (Nikon, Japan) at 10X magnification at different time points.

In ovo chick chorioallantoic membrane (CAM) assay

In ovo CAM assay was performed to study the angiogenesis according to the protocol mentioned earlier [32]. Briefly, fertilized eggs of chick RIR (Rhode Island Red) breed were purchased from Central Poultry Development Organization (CPDO, Bhubaneswar). Eggs were incubated in a humidified atmosphere at 37°C and after 60h from fertilisation time, a window was made in the egg shell. Two sets of eggs were used in this experiment. In the first set of eggs, the CAM membranes were exposed to different types of CM (100 µg per 5 ml egg fluid) on a sterilized filter. On the other hand, in the other set of eggs, CAM membranes were exposed to CM of QC treated cancer cells (cells were treated with the respective IC_{50} values of QC). Both the sets of eggs were incubated for another 24 h. The changes in vascularisation in CAM were studied and pictures were taken photographically. Graphical presentation of average vascularization on CAM membrane was analysed using AngioTool software (NIH). The graphical representation was made with GraphPad Prism 5.0 software.

Tubulogenesis assay in HUVECs to check tube formation

Tube formation assay was performed in HUVECs according to the protocol described earlier [31]. Briefly, $2x10^3$ HUVECs were seeded in 24 well matrigel coated plate and then two sets of HUVECs were used in this experiment. In the first set, the HUVECs were exposed to different types of CM (100 µg/ 3ml, contains most of angiogenic stimuli). On the other hand, other set of HUVECs were exposed to CM of QC treated cancer cells (cells were treated with the respective IC_{50} values of QC). Both the sets HUVECs were incubated for another 48 h. To clearly visualise the tube-like structure it was stained with acridine orange.

Photos were captured from different microscopic fields at 40X magnification (Evos Fluorescence Microscope, Thermo Fisher Scientific, MA, USA). Average tube-lengths were analysed by using AngioTool software (NIH). The graphical representation was made with GraphPad Prism 5.0 software.

Gelatin Zymography to check the expression of matrix metallopeptidases

As previously reported protocol, gelatin zymography was performed to check the extracellular matrix metallopeptidase (MMP-9 and MMP-2) activity [32]. Briefly, gelatin works as a substrate for MMP-9 and MMP-2 which are gelatinase in nature. In the first set, 1 $\times 10^6$ HUVECs alone and CM supplemented were grown in 6-well plate for 48 h and in another set, QC was added in the similar panel as the first set just to check the effect of QC. Then the supernatant was collected and each sample loaded with 40µg of protein was separated on SDS-PAGE containing gelatin co-polymerized with polyacrylamide gel to detect MMP-9 and MMP-2 expression. After that, gels were washed twice with washing buffer (2.5% Triton X-100, 5 mM $CaCl_2$, 50 mM Tris HCL, 1 µM $ZnCl_2$ in dH_2O), incubated at 37°C shaker incubator with incubation buffer (1% Triton X-100, 5 mM $CaCl_2$, 50 mM Tris HCL, 1 µM $ZnCl_2$ in dH_2O) for 16–21 h and stained with 1% CBBR-250. After destaining the gels in the destaining solution, the regions, where MMP-9 and MMP-2 acted, appeared as white bands in contrast to the dark background.

Immunofluorescence assay

Intracellular phospho-cMET (Y1234 & Y1356) was detected using fluorescence-based immunocytochemistry according to our previous method [33]. In brief, MDA-MB-231PEMT cells were seeded on coverslips and treated with QC for 24 h. Next, the cells were fixed with acetone:methanol (1:1,v/v) for 15 mins at -20°C. After fixation and blocking, the cells were incubated overnight with the respective primary antibody at 4˚C followed by washing with 1XPBS. Then TRIT-C conjugated secondary antibody was added and incubated for 2 h at room temperature (RT). After washing twice with 1XPBS, nuclei were counterstained with DAPI. The images were taken using an inverted fluorescence microscope (Nikon, Tokyo, Japan) at 20X magnification.

Effect of QC in tumor regression, metastasis and angiogenesis by using Xenograft mice model

Tumor induction in mice and all related experiments were performed as per the protocol discussed previously [33]. Briefly, the Institutional Animal Ethical Committee approved all the animal work and experimental protocols (IAEC, KIIT Deemed to be University, Bhubaneswar, India). Tumor induction at the site of breast fat pads of the mice was performed. Briefly, 6-7 weeks old female BALB/c mice were taken for the experiments. PEMT cells developed from breast cancer primary cells(1×10^7 in 200 µL of freshly prepared sterile PBS) were injected into the right mammary fat pads of the animals. After tumor formation the tumor containing mice were treated with QC (20 mg/kg/ day for each treatment condition) for 15 days by oral administration with a feeding needle. The animals were physically monitored for their health, body weight and tumor growth, etc. After treatment the animals were sacrificed and the samples (breast fat pad including tumor) were collected for experimentations.

Immunohistochemistry (IHC) of mice and patient tumor tissues

H&E staining and IHC were performed as per protocol described previously [35]. Briefly, paraffin-embedded specimens were sectioned (at 5 μm thick) then mounted on charged slides. After heating the slides at 60 °C for 30–40 min, de-waxed with xylene and rehydrated by immersing in decreasing series of alcohols concentration (100%, 90% and 70%, respectively). The sections were immersed into haematoxylin followed by eosin stain and washed in rinsing water. After that the sections were dehydrated by dipping in increasing concentrations of alcohol (70%, 90%, and 100%) followed by xylene and acetone for 2 min each. Then the slides were mounted with DPX and coverslips. The images were taken in a brightfield microscope at 20X magnification (Leica DM200, USA).

In IHC, rehydrated tissue sections (3 μm thick) were washed in 1X PBS, and then the antigen was retrieved by citric acid buffer (pH 6). After that, nonspecific sites and endogenous peroxide activity were blocked in the slide by 5% foetal bovine serum (FBS) and hydrogen peroxide. Then the sections were incubated with respective primary antibodies at 4 °C for overnight. The primary antibody was taken out and washed 3 times with 1X PBS. Next, the slides were incubated with HRP-conjugated secondary antibody at room temperature for 1h. Then slides were washed with 1X PBS and immunoreactivity was observed using 3,3-Diaminobenzidine (DAB) peroxidase substrate kit (SK-4100, Vector Laboratories, CA, USA) followed by counterstain with haematoxylin. The sections were mounted with DPX and left for dry. The images were taken at 20X magnification using a brightfield microscope (Leica DM200, USA).

Statistical analysis

The given images and data was one of the representatives of three independent experiments. Statistical analysis was carried out using Graph Pad Prism 5.0 software (USA). Results represented here were the mean±standard deviation (SD) of three independent experiments. Data were analysed using one-way ANOVA followed by Bonferroni's all pair comparison test. Statistical significance was designated as 'ns' (non-significant, $P>0.05$), along with '$*$' $P < 0.05$, '$**$' $P < 0.005$ and '$***$' $P < 0.0001$ represent significant data.

Declarations

STUDY APPROVAL

Mice were used for experimental purposes according to the rules and regulations of CPCSEA, New Delhi after the approval (Ethical clearance approval Regd. #1577/PO/Re/S/2011/CPCSEA) of Institutional Animal Ethics Committee (IAEC), KIIT University.

All the patient samples were procured and used following all necessary guidelines after getting the approval of the Institutional Ethics Committee (Ethical clearance approval Regd. #ECR/297/Inst/OR/2013) from Acharya Harihar Regional Cancer Centre, Cuttack, Odisha, India.

ACKNOWLEDGEMENTS

This work was supported by ICMR, Govt. of India.

AUTHOR CONTRIBUTIONS

BD performed the majority of the experiments and wrote the initial draft of the Manuscript. CS, SC, SRD, SS, and SP performed some of the experiments and helped to do statistical analysis. KG provided patient samples. CNK conceived the idea, planned the experiments, and wrote the final version of MS.

FUNDING

Partial financial support was received from Indian Council of Medical Research (ICMR), Govt. of India for conducting this research work.

DATA AVIALABILITY STATEMENT

The datasets generated during and/or analysed during the current study are available from the corresponding author on request.

Conflict of interest: The authors declare that they have no conflict of interest.

References

1. DeSantis CE, Ma J, Gaudet MM, et al (2019) Breast cancer statistics, 2019. CA Cancer J Clin 69:438–451. https://doi.org/10.3322/caac.21583
2. Song K, Farzaneh M (2021) Signaling pathways governing breast cancer stem cells behavior. Stem Cell Res Ther 12:245. https://doi.org/10.1186/s13287-021-02321-w
3. Ahmad A (2013) Pathways to Breast Cancer Recurrence. ISRN Oncol 2013:290568. https://doi.org/10.1155/2013/290568
4. Saeg F, Anbalagan M (2018) Breast cancer stem cells and the challenges of eradication: a review of novel therapies. Stem Cell Investig 5:39. https://doi.org/10.21037/sci.2018.10.05
5. Krishnapriya S, Sidhanth C, Manasa P, et al (2019) Cancer stem cells contribute to angiogenesis and lymphangiogenesis in serous adenocarcinoma of the ovary. Angiogenesis 22:441–455. https://doi.org/10.1007/s10456-019-09669-x
6. Huang R, Rofstad EK (2017) Cancer stem cells (CSCs), cervical CSCs and targeted therapies. Oncotarget 8:35351–35367. https://doi.org/10.18632/oncotarget.10169
7. Ayob AZ, Ramasamy TS (2018) Cancer stem cells as key drivers of tumour progression. J Biomed Sci 25:20. https://doi.org/10.1186/s12929-018-0426-4
8. Tchou J, Zhao Y, Levine BL, et al (2017) Safety and Efficacy of Intratumoral Injections of Chimeric Antigen Receptor (CAR) T Cells in Metastatic Breast Cancer. Cancer Immunol Res 5:1152–1161. https://doi.org/10.1158/2326-6066.CIR-17-0189

9. Gaule PB, Crown J, O'Donovan N, Duffy MJ (2014) cMET in triple-negative breast cancer: is it a therapeutic target for this subset of breast cancer patients? Expert Opin Ther Targets 18:999–1009. https://doi.org/10.1517/14728222.2014.938050
10. Puccini A, Marín-Ramos NI, Bergamo F, et al (2019) Safety and Tolerability of c-MET Inhibitors in Cancer. Drug Saf 42:211–233. https://doi.org/10.1007/s40264-018-0780-x
11. The clinical and functional significance of c-Met in breast cancer: a review - PubMed. https://pubmed.ncbi.nlm.nih.gov/25887320/. Accessed 20 Dec 2021
12. Motomura H, Nozaki Y, Onaga C, et al (2020) High Expression of c-Met, PKCλ and ALDH1A3 Predicts a Poor Prognosis in Late-stage Breast Cancer. Anticancer Res 40:35–52. https://doi.org/10.21873/anticanres.13924
13. Mitra S, Bal A, Kashyap D, et al (2020) Tumour angiogenesis and c-Met pathway activation - implications in breast cancer. APMIS Acta Pathol Microbiol Immunol Scand 128:316–325. https://doi.org/10.1111/apm.13031
14. Das B, Kundu CN (2021) Anti-Cancer Stem Cells Potentiality of an Anti-Malarial Agent Quinacrine: An Old Wine in a New Bottle. Anticancer Agents Med Chem 21:416–427. https://doi.org/10.2174/1871520620666200721123046
15. Oien DB, Pathoulas CL, Ray U, et al (2021) Repurposing quinacrine for treatment-refractory cancer. Semin Cancer Biol 68:21–30. https://doi.org/10.1016/j.semcancer.2019.09.021
16. de Souza PL, Castillo M, Myers CE (1997) Enhancement of paclitaxel activity against hormone-refractory prostate cancer cells in vitro and in vivo by quinacrine. Br J Cancer 75:1593–1600. https://doi.org/10.1038/bjc.1997.272
17. Quinacrine and curcumin synergistically increased the breast cancer stem cells death by inhibiting ABCG2 and modulating DNA damage repair pathway - PubMed. https://pubmed.ncbi.nlm.nih.gov/31877386/. Accessed 20 Dec 2021
18. Oien DB, Pathoulas CL, Ray U, et al (2021) Repurposing quinacrine for treatment-refractory cancer. Semin Cancer Biol 68:21–30. https://doi.org/10.1016/j.semcancer.2019.09.021
19. Dash SR, Chatterjee S, Sinha S, et al (2021) NIR irradiation enhances the apoptotic potentiality of quinacrine-gold hybrid nanoparticles by modulation of HSP-70 in oral cancer stem cells. Nanomedicine Nanotechnol Biol Med 102502. https://doi.org/10.1016/j.nano.2021.102502
20. Siddharth S, Nayak D, Nayak A, et al (2016) ABT-888 and quinacrine induced apoptosis in metastatic breast cancer stem cells by inhibiting base excision repair via adenomatous polyposis coli. DNA Repair 45:44–55. https://doi.org/10.1016/j.dnarep.2016.05.034
21. Bouattour M, Raymond E, Qin S, et al (2018) Recent developments of c-Met as a therapeutic target in hepatocellular carcinoma. Hepatology 67:1132–1149. https://doi.org/10.1002/hep.29496
22. Mo H-N, Liu P (2017) Targeting MET in cancer therapy. Chronic Dis Transl Med 3:148–153. https://doi.org/10.1016/j.cdtm.2017.06.002
23. Guo C, Stark GR (2011) FER tyrosine kinase (FER) overexpression mediates resistance to quinacrine through EGF-dependent activation of NF-κB. Proc Natl Acad Sci U S A 108:7968–7973.

https://doi.org/10.1073/pnas.1105369108

24. Parekh A, Das D, Das S, et al (2018) Bioimpedimetric analysis in conjunction with growth dynamics to differentiate aggressiveness of cancer cells. Sci Rep 8:783. https://doi.org/10.1038/s41598-017-18965-9
25. Hanahan D, Weinberg RA (2011) Hallmarks of cancer: the next generation. Cell 144:646–674. https://doi.org/10.1016/j.cell.2011.02.013
26. Zhang Y, Xia M, Jin K, et al (2018) Function of the c-Met receptor tyrosine kinase in carcinogenesis and associated therapeutic opportunities. Mol Cancer 17:45. https://doi.org/10.1186/s12943-018-0796-y
27. Prognostic significance of c-Met in breast cancer: a meta-analysis of 6010 cases - PubMed. https://pubmed.ncbi.nlm.nih.gov/26047809/. Accessed 20 Dec 2021
28. Parr C, Jiang WG (2001) Expression of hepatocyte growth factor/scatter factor, its activator, inhibitors and the c-Met receptor in human cancer cells. Int J Oncol 19:857–863
29. Wang Y, Zhan Z, Jiang X, et al (2016) Simm530, a novel and highly selective c-Met inhibitor, blocks c-Met-stimulated signaling and neoplastic activities. Oncotarget 7:38091–38104. https://doi.org/10.18632/oncotarget.9349
30. SURVIVIN as a marker for quiescent-breast cancer stem cells-An intermediate, adherent, pre-requisite phase of breast cancer metastasis - PubMed. https://pubmed.ncbi.nlm.nih.gov/27411340/. Accessed 20 Dec 2021
31. Nanoformulated quinacrine regulates NECTIN-4 domain specific functions in cervical cancer stem cells - PubMed. https://pubmed.ncbi.nlm.nih.gov/32603697/. Accessed 20 Dec 2021
32. Chatterjee S, Sinha S, Molla S, et al (2021) PARP inhibitor Veliparib (ABT-888) enhances the anti-angiogenic potentiality of Curcumin through deregulation of NECTIN-4 in oral cancer: Role of nitric oxide (NO). Cell Signal 80:109902. https://doi.org/10.1016/j.cellsig.2020.109902
33. Pradhan R, Chatterjee S, Hembram KC, et al (2021) Nano formulated Resveratrol inhibits metastasis and angiogenesis by reducing inflammatory cytokines in oral cancer cells by targeting tumor associated macrophages. J Nutr Biochem 92:108624. https://doi.org/10.1016/j.jnutbio.2021.108624
34. Nayak A, Das S, Nayak D, et al (2019) Nanoquinacrine sensitizes 5-FU-resistant cervical cancer stem-like cells by down-regulating Nectin-4 via ADAM-17 mediated NOTCH deregulation. Cell Oncol Dordr 42:157–171. https://doi.org/10.1007/s13402-018-0417-1
35. Clinical significance of a pvrl 4 encoded gene Nectin-4 in metastasis and angiogenesis for tumor relapse - PubMed. https://pubmed.ncbi.nlm.nih.gov/31617074/. Accessed 20 Dec 2021

Figures

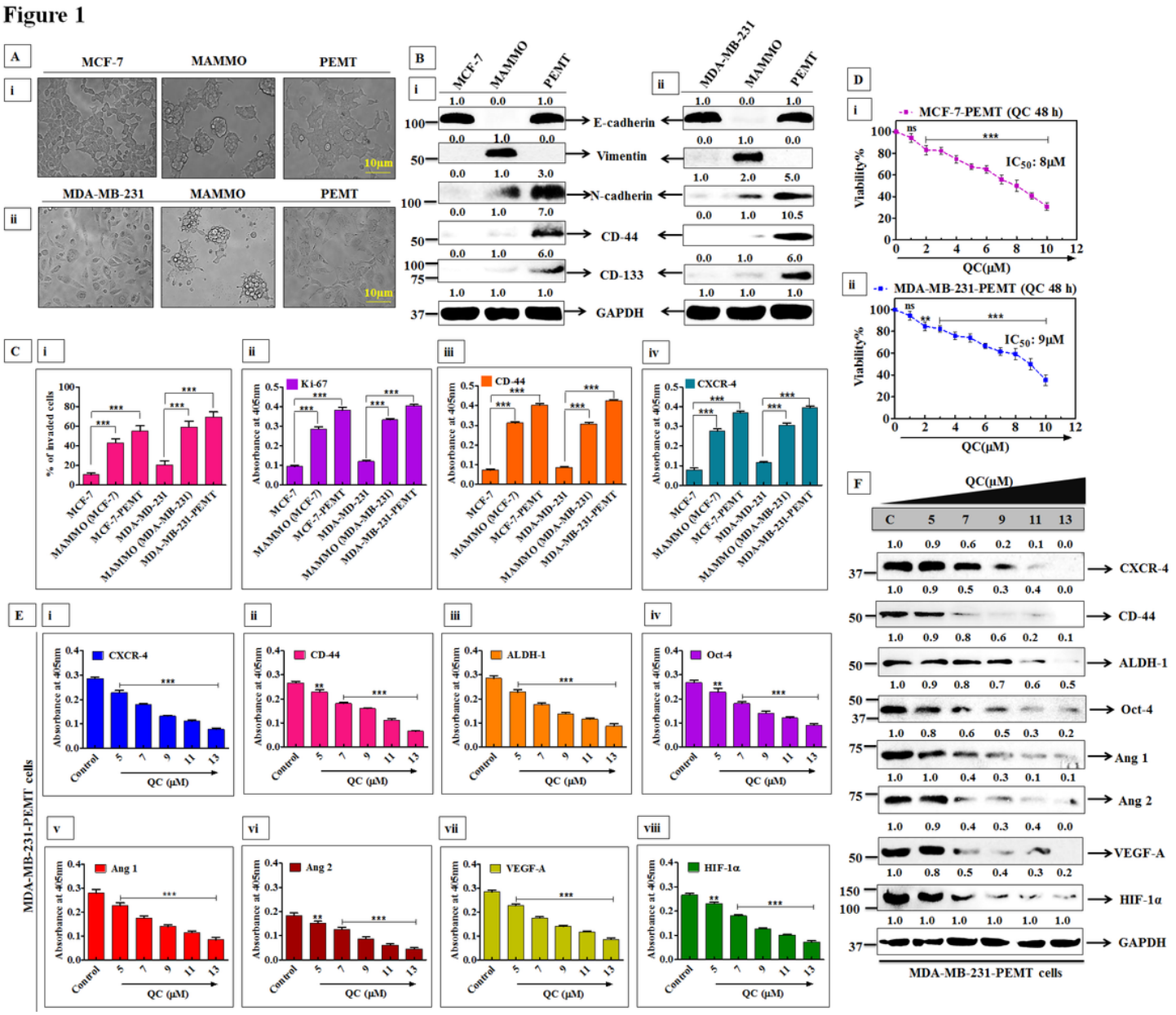

Figure 1

Effect of QC in regulation of metastasis and angiogenesis in PEMT cells.

A Morphology of metastatic model at different stages **(i & ii)**. **B** Validation of metastatic model **(i & ii)**. **C** Matrigel invasion assay **(i).** The expression of proliferation marker Ki-67 (**ii**), metastatic and CSCs marker CD-44 **(iii),** and CXCR-4 **(iv)** in metastatic models was measured by ELISA. **D** IC_{50} of QC in MCF-7-PEMT **(i)** MDA-MB-231-PEMT **(ii**) cells. **E** Expression of some representative metastatic markers **(i-iv)** and angiogenic regulators **(v-viii)** in MDA-MB-231-PEMT cells after QC treatment were measured by ELISA. **F** Expression of representative metastasis and angiogenesis markers in MDA-MB-231-PEMT cells after QC treatment were checked by western blot analysis.

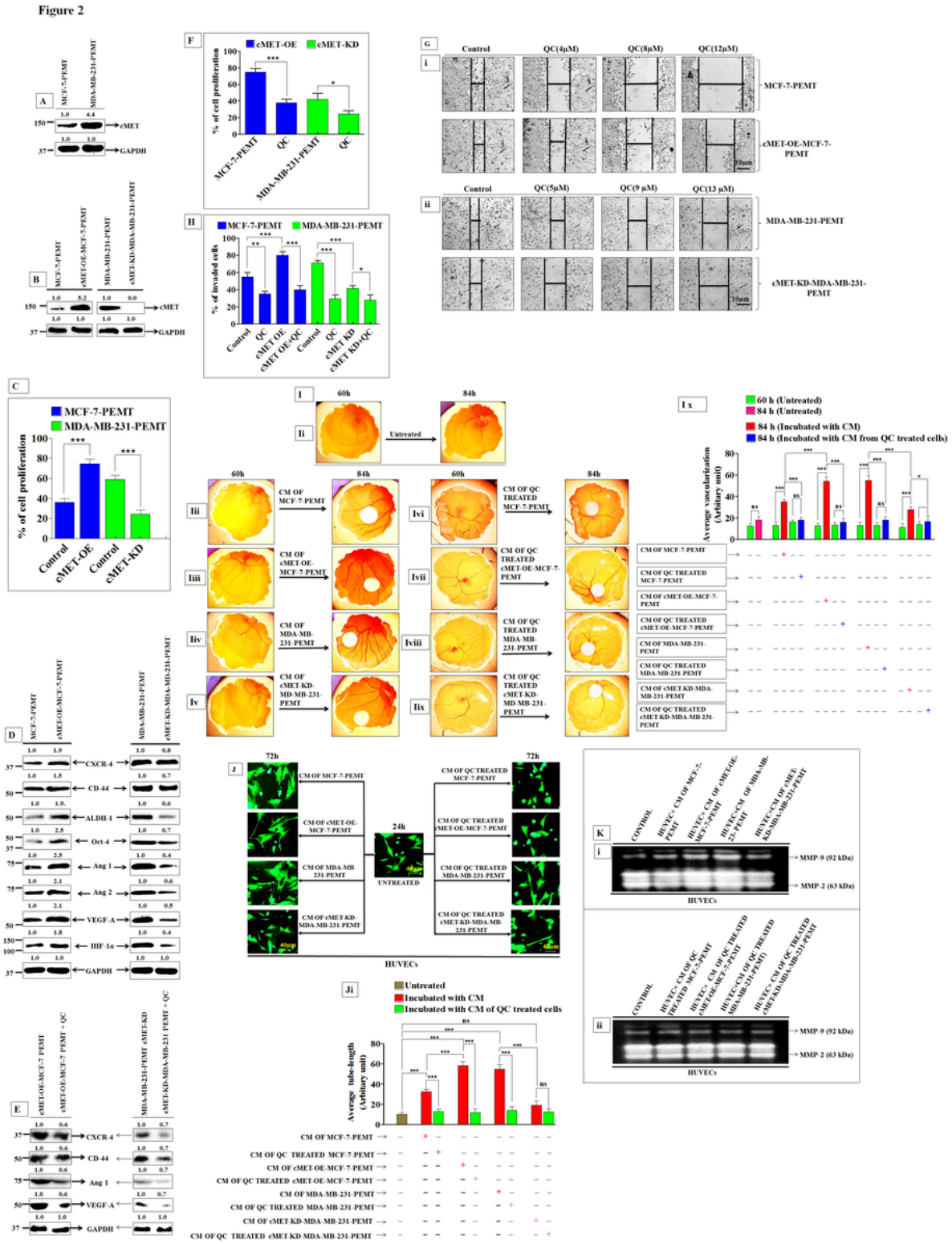

Figure 2

cMET mediated metastasis and angiogenesis is inhibited by QC.

A Comparative expression of cMET. **B** Overexpression of cMET in MCF-7-PEMT cells and knockdown of cMET in MDA-MD-231 PEMT cells. **C** Cell proliferation assay. **D** Expression of representative metastasis and angiogenic regulators. **E** Expression of representative metastasis and angiogenesis markers upon QC

treatment. **F** Percentage of cell proliferation after QC treatment. **G** Wound healing potentiality of cMET-OE-MCF-7-PEMT cells **(i)** and cMET-KD-MDA-MB-231-PEMT cells **(ii)** upon QC treatment. **H** Invasive potentiality of the cells with and without QC treatment. **I** *In ovo* CAM assay **(Ii-ix)** Graphical presentation of average vascularization on CAM **(Ix)**. **J** *In vitro* tube formation assay. The graphical representation of average tube length **(Ji). K** Gelatin zymography to check the expression of MMP-9, and MMP-2 after incubating with different CMs in HUVECs **(i)** and effect of QC treatment **(ii)**.

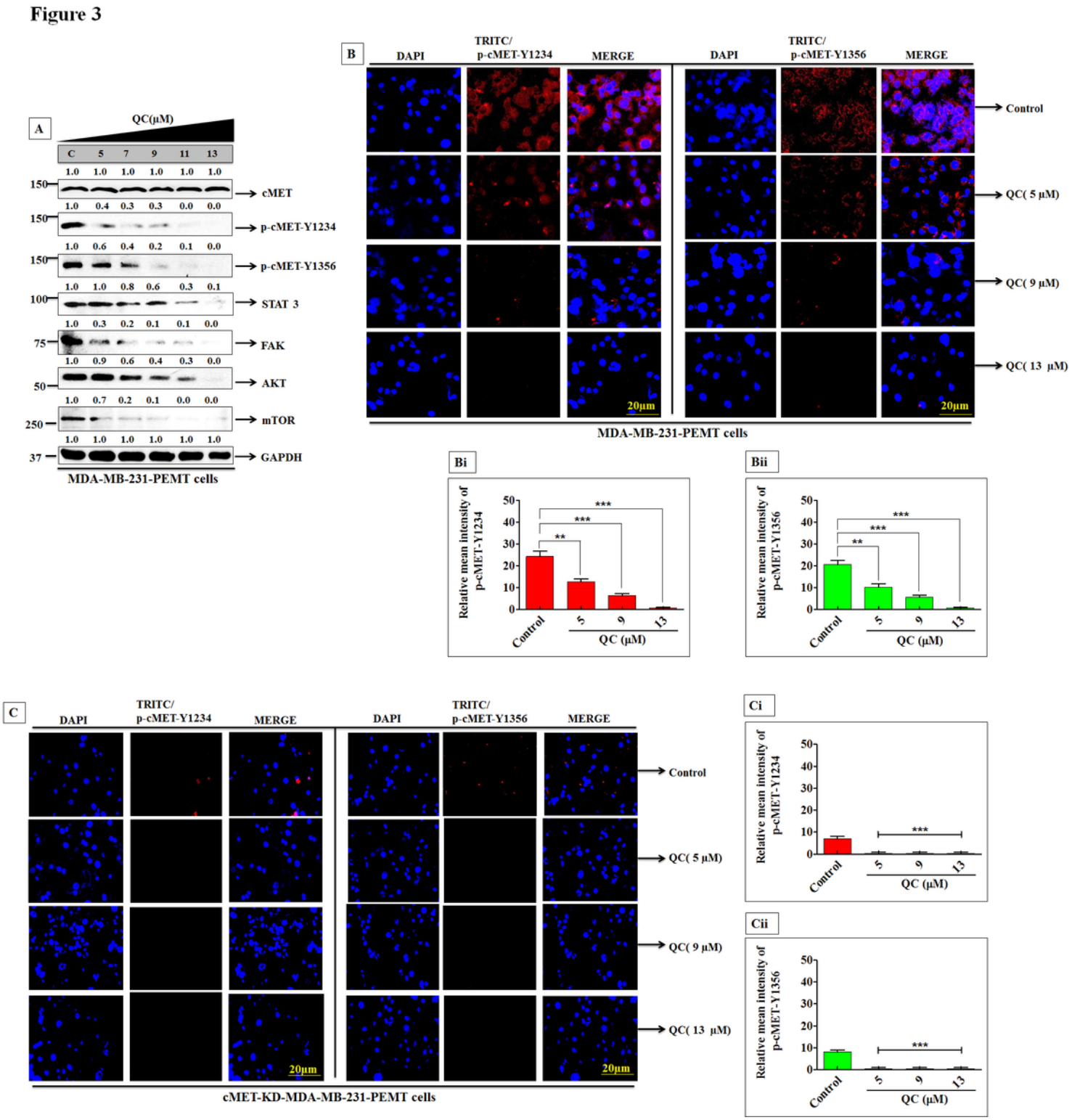

Figure 3

Molecular mechanism of QC mediated inhibition of cMET and its downstream targets.

A Expression of cMET, p-cMET (Y1234 & 1356) and downstream proteins of cMET after QC treatment. **B** Immunocytochemical staining of phospho-cMET domains (Y1234 & Y1356) after QC treatment in MDA-MB-231-PEMT cells. **Bi & Bii** Bar graph represents relative mean intensity of p-cMET-Y123) and p-cMET-

Y1356. **C** Immunocytochemical staining of phospho-cMET domains (Y1234 & Y1356) after QC treatment in MDA-MB-231-PEMT-cMET-KD cells. **Ci & Cii** Bar graph represents relative mean intensity of p-cMET-Y1234 and p-cMET-Y1356.

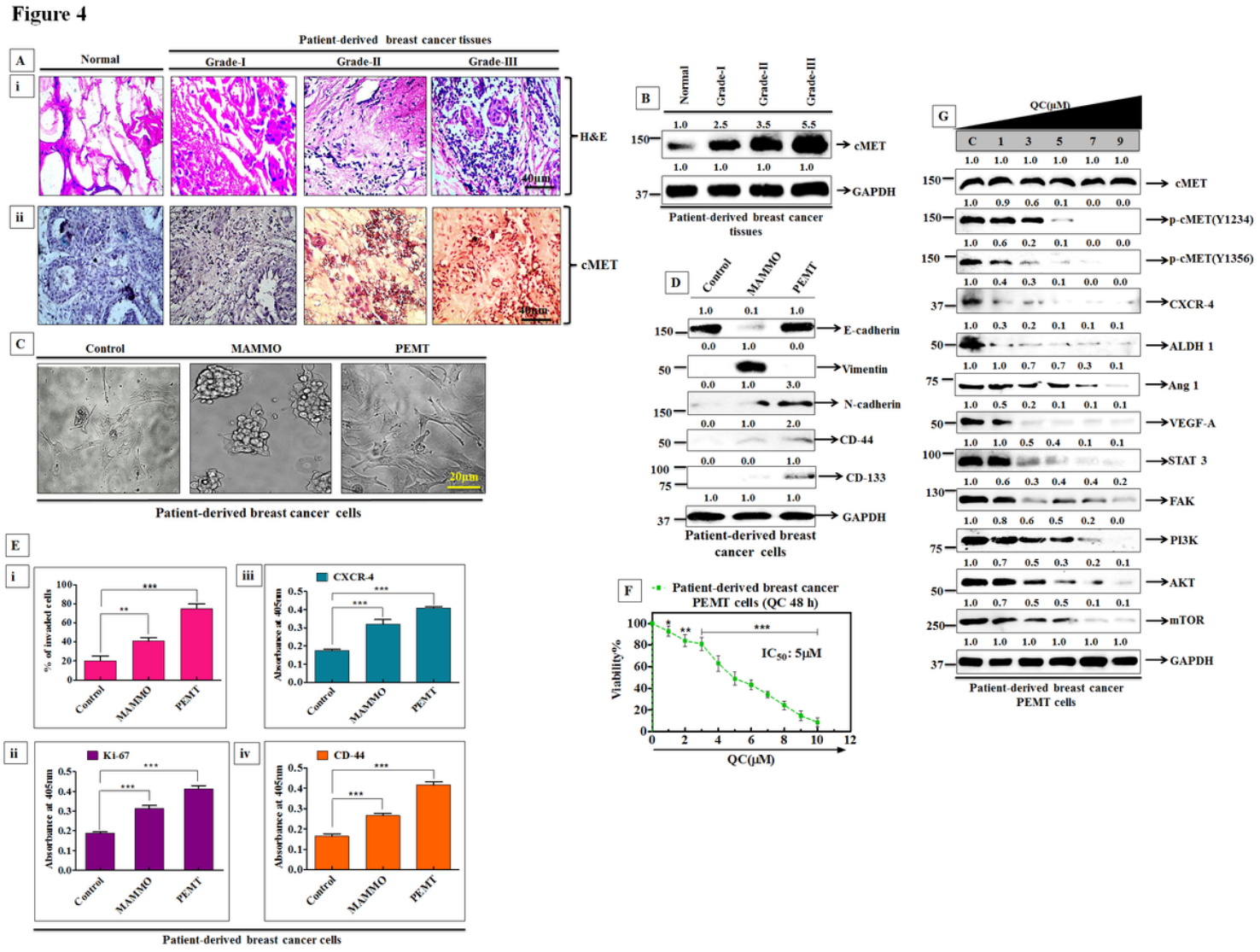

Figure 4

Effect of QC on cMET-mediated metastasis and angiogenesis in patient-derived breast cancer PEMT cells.

A H&E staining of normal and different grades (I–III) of breast cancer tissue **(i)**. Expression of cMET was analysed by IHC **(ii)**. **B** Expression of cMET in different grades of human breast tumor tissue. **C** Morphology of different stages of metastatic model in patient-derived breast tumor cells. **D** The expression of representative metastatic and stemness markers was measured in metastatic model of patient-derived breast cancer cells. **E.** Matrigel invasion assay **(i)**, The expression of Ki-67 **(ii)**, CXCR-4 **(iii).** and CD-44 marker was measured by ELISA **(iv)**. **F** Cell viability assay. **G** Expression of cMET, phospho-

cMET, representative metastasis, angiogenesis markers and downstream signaling proteins of cMET were assessed after treatment with increasing concentrations of QC in patient-derived breast cancer PEMT cells.

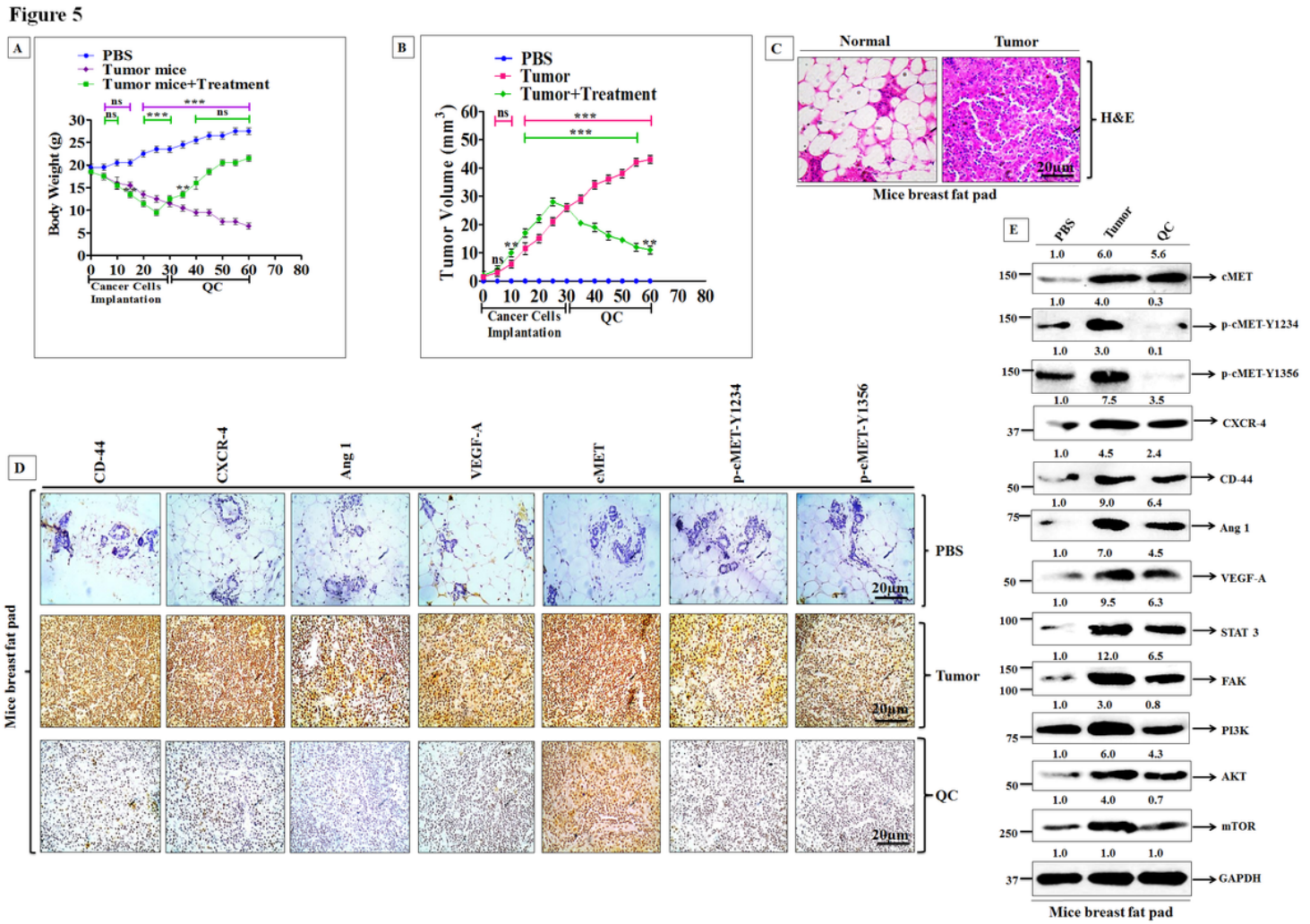

Figure 5

QC reduces the metastasis and angiogenesis in mice xenograft model.

A Graph representing the average body weight of mice before and after the treatment with QC. **B** Graph representing the average tumor volume of mice. **C** H&E staining of normal and cancer breast fat pad tissue of mice. **D** Immunohistochemical expression of Ang1, VEGF-A, CD-44, CXCR-4, cMET, and phospho-cMET (Y1234 & Y1356) in different tumor tissues with and without (only PBS) the treatment of QC. **E** Expression of cMET, phospho-cMET, representative metastasis, and angiogenesis markers, and downstream signaling proteins of cMET.

Figure 6

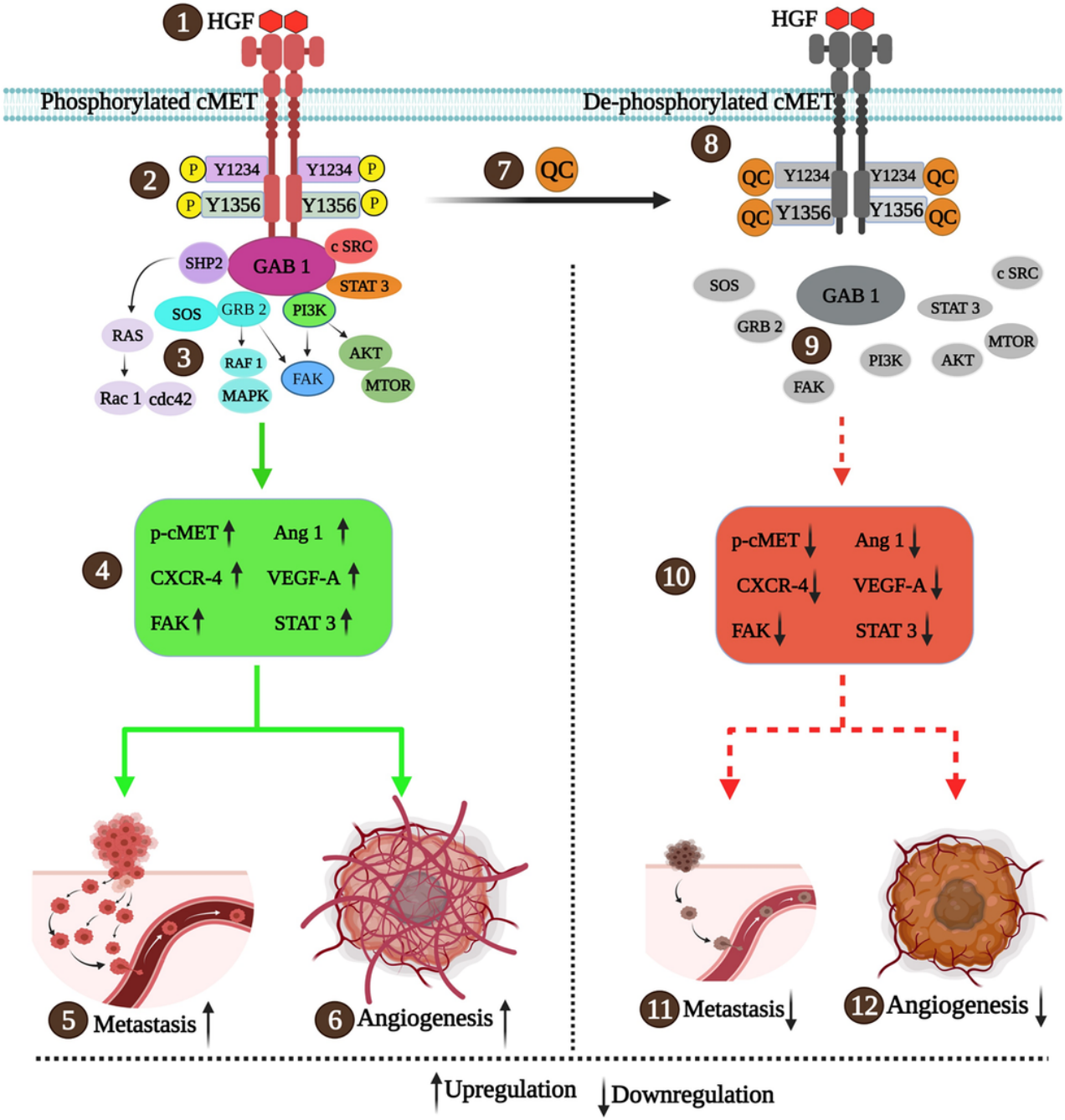

Figure 6

Schematic diagram depicting the deregulation of cMET-mediated metastasis and angiogenesis by QC by targeting phospho-cMET.

1 Binding of HGF as specific ligand allows receptor dimerization and activation of cMET. **2** Activation of cMET occurs through the phosphorylation of tyrosine kinase domain of cMET (Y1234 and Y1356). **3 & 4** Phosphorylation of cMET upregulates other downstream signaling proteins of cMET as well as several metastatic and angiogenesis markers. **5 & 6** Induction of metastasis and angiogenesis processes. **7 & 8**

QC treatment dephosphorylates cMET. **9** Dephosphorylation leads to inactivation of whole downstream signaling cascade. **10** QC downregulates the downstream signaling proteins of cMET as well as different metastatic and angiogenesis markers. **11 & 12** As a result significant reduction of metastasis and angiogenesis processes take place **(Created with BioRender.com)**

Supplementary Files

This is a list of supplementary files associated with this preprint. Click to download.

- GraphicalAbstract.jpeg